Archives of Mining Sciences 46, 1 (2001) 19–36

STANISŁAW WOLNY *

THEORETICAL AND EXPERIMENTAL ANALYSIS OF LOADS IN MINING TUB SUSPENSIONS IN THE CONDITION OF OPERATIONAL BRAKING OF A MINE HOIST FACILITY

TEORETYCZNA I DOŚWIADCZALNA ANALIZA OBCIĄŻEŃ W ZAWIESZENIACH NACZYŃ WYDOBYWCZYCH W WARUNKACH HAMOWANIA MANEWROWEGO GÓRNICZEGO URZĄDZENIA WYCIĄGOWEGO

The paper presents the results of a dynamic analysis of a mine hoist in the operational braking condition. Particular emphasis is placed on the analytical determination of incurred loadings in mining tub suspensions in comparison with the results obtained in actual practice.

Key words: mine hoist, incurred loadings, dynamic analysis, braking condition.

Obowiązujące obecnie kryteria wymiarowania i projektowania elementów naczynia wydobywczego nie odzwierciedlają pełnej specyfiki pracy górniczego urządzenia wyciągowego. Stosowana metoda naprężeń dopuszczalnych umożliwia jedynie ocenę ich nośności, nie daje natomiast możliwości określenia ich trwałości zmęczeniowej.

Potrzebę nowelizacji metod obliczeń wytrzymałościowych elementów urządzenia wyciągowego stwierdzono już przed kilkunastu laty, czemu towarzyszyło podjęcie szeregu prac teoretycznych i badawczych między innymi (Gerlich & Horstman, 1993), (Knop, 1975) w zakresie identyfikacji ich obciążenia. Wykazano istotną rozbieżność wartości obciążeń rzeczywistych do przyjmowanych na podstawie obowiązujących wytycznych (aktualnie Załącznik, 1995), zwłaszcza przy wzroście udźwigu, prędkości oraz głębokości ciągnienia.

Podsumowując można stwierdzić, że pomimo różnego rodzaju prób rozwiązania tego problemu, obliczenia wytrzymałościowe elementów naczynia wydobywczego (zawieszenia,

* WYDZIAŁ INŻYNIERII MECHANICZNEJ I ROBOTYKI, AKADEMIA GÓRNICZO-HUTNICZA, 30-059 KRAKÓW, AL. MICKIEWICZA 30

głowica, rama dolna, cięgna) w dalszym ciągu wykazują pewne braki, wśród których jako zasadnicze wymienić można:

a) maksymalne naprężenia w elementach naczynia wydobywczego określa się uwzględniając tylko obciążenia statyczne,

b) w naczyniu wydobywczym, jako konstrukcji przestrzennej wyróżnia się elementy, zastępując je schematami obliczeniowymi (pręty rozciągane, belki swobodnie podparte) znacznie odbiegającymi od rzeczywistości,

c) obowiązuje metoda naprężeń dopuszczalnych, a w bardzo ograniczonym zakresie ocenia się wytrzymałość zmęczeniową.

Mając powyższe na uwadze, koniecznym jest podjęcie prac nad opracowaniem nowych kryteriów umożliwiających wymiarowanie i ocenę bezpieczeństwa elementów naczynia wydobywczego.

Osiągnięcie tego celu wymagać będzie:

1. określenia wartości obciążeń elementów naczynia wydobywczego w czasie normalnej eksploatacji jak i dla stanów awaryjnych na podstawie przeprowadzonej analizy dynamicznej, zweryfikowanych pomiarami na obiekcie rzeczywistym,

2. przeprowadzenia analizy wytrzymałościowej wybranych elementów i węzłów naczynia wydobywczego,

3. opracowania kryteriów oceny przydatności wybranych elementów naczynia wydobywczego w aspekcie obniżenia masy i przedłużenia okresu bezpiecznej ich eksploatacji.

Rozważania zawarte w tym opracowaniu koncentrują się na części punktu 1, a dotyczą wyników analizy dynamicznej pracy górniczego urządzenia wyciągowego w warunkach hamowania manewrowego. Szczgółowym badaniom poddano obciążenia zawieszeń naczyń wydobywczych, na tle wyników eksperymentu przeprowadzonego na obiekcie rzeczywistym.

Ograniczając się do najbardziej interesującego dla praktyki ruchowej przypadku położenia naczyń wydobywczych, jak na rysunku 1, gdy jedno z nich znajduje się w okolicy nadszybia, a drugie w okolicy podszybia (hamowanie przy dojeździe do nadszybia) wyciąg zastąpiono modelem jak na rysunku 2. Dla przyjętego modelu zapisano równania ruchu elementów lin (nośnych i wyrównawczych) jak dla cięgna sprężystego (3). Odcinek lin nośnych między naczyniem (pełnym) dojeżdżającym do górnego poziomu załadowczego a kołem pędnym zastąpiono sprężyną o współczynniku sprężystości równym sprężystości tego odcinka lin.

Wykorzystując rozwiązanie równania falowego podano wzory określające przemieszczenia dowolnych przekrojów poprzecznych lin nośnych (7a) i wyrównawczych (7b) w tym zawieszeń naczyń i lin, jako funkcji siły hamującej oraz parametrów ruchowych wyciągu. Ponadto podano wzory w postaci zamkniętej na naprężenia w dowolnych przekrojach lin.

Uzyskane na drodze teoretycznej rezultaty, charakteryzujące proces hamowania manewrowego, zostały zweryfikowane drogą pomiarów wybranych wielkości na obiekcie rzeczywistym. Eksperyment — z uwagi na trudności natury technicznej — ograniczono do pomiaru sił w zawieszeniu naczynia pełnego dojeżdżającego do górnego poziomu załadowczego, hamowanego przy użyciu hamulca manewrowego.

Wyniki wykonanych pomiarów korespondują z wynikami przeprowadzonych symulacji opartych na rezultatach przeprowadzonej analizy dynamicznej. Różnica w przebiegach czasowych mierzonych i wyznaczonych na drodze teoretycznej wartości wielkości charakteryzujących proces hamowania manewrowego — sił w zawieszeniach naczyń — w skrajnych wypadkach nie przekracza kilku procent (vide wykresy rys. 7, rys. 8).

Uzyskane rezultaty stanowią materiał wyjściowy do właściwego opisu funkcji obrazującej zmianę obciążenia elementów naczynia wydobywczgo podczas hamowania manewrowego jako parametrów układu jak i urządzenia hamującego. Zależności te są niezbędne do właściwego zaprojektowania między innymi sprzężenia ciernego liny z kołem pędnym a ponadto stanowią jeden z podstawowych czynników koniecznych do opracowania kryteriów wymiarowania i projektowania elementów naczynia wydobywczgo w aspekcie podwyższenia bezpieczeństwa i niezawodności ich pracy.

Słowa kluczowe: wyciąg kopalniany, dynamika, hamowanie, pomiary obciążeń.

1. Introduction

Mining tubs have to be hauled on the carcass of the shaft to the area of unloading (or loading). The shaft tower is constructed in such a way that these operations may be performed. The structure also contains elements that support rope wheels and in some designs, the complete hoisting mechanism. Fig. 1 shows the scheme of a typical winding gear tower installation as used in Poland.

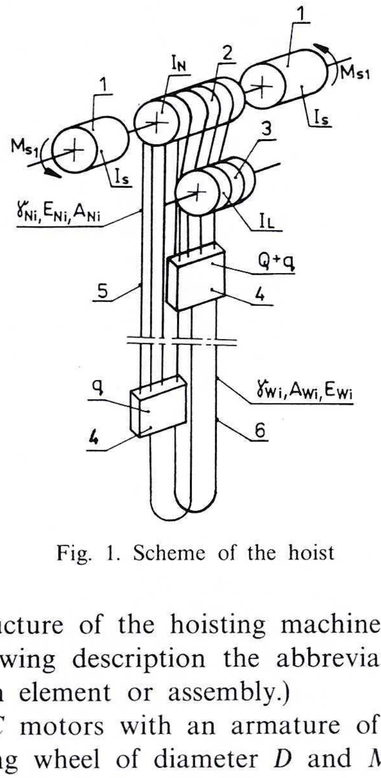

Fig. 1. Scheme of the hoist

The technological structure of the hoisting machine illustrated on this figure comprises: (In the Following description the abbreviation *M.I.* — denotes the Moment of Inertia of an element or assembly.)

1 — slow-running *DC* motors with an armature of $M.I.I_s$,
2 — multi-rope driving wheel of diameter D and $M.I.I_N$,
3 — the set of deflecting wheels of $M.I.I_L$,
4 — skip tubs of mass q and the load capacity Q with the upper tub filled,
5 — parallel lines of supporting ropes of linear density γ_N under tension rigidity $(A_W E_W)$,
6 — parallel lines of counterbalance ropes of the linear density γ_N under tension rigidity $A_W E_W$.

The rotors of the driving motors and the drive wheel, connected by the short rigid shaft are in rotary motion. Moreover in the rotary motion, elements of the supporting ropes, are in motion with the driving wheel in a semicircular arc. The skip tubs, as well as supporting and the counterbalance ropes are in reciprocal motion.

These considerations will be restricted to one stage of the facility of the operation, namely the operational braking, as this process highly hazardous situations for operational reliability, which may cause a failure of the frictional connection between the rope and the drive wheel (Knop, 1975), (Gerlich & Horstmann, 1993), (Wolny, 2000 a).

The characteristic feature of mine winding machinery is the distribution of the mechanical components between the hoisting machinery and the bottom of the shaft. Furthermore they are distributed unequally throughout the system. Rotating masses, which form a considerable component in the total mass of the hoist, are located in the tower and masses of both parts of supporting and balance ropes are located within the depth of the shaft. Disproportion in the mass distribution will be once more increased (Wolny, 2000 a), when a full mining tub reaches the surface. Therefore, for deep and medium depths of extraction by means of winding gear it would be reasonable to consider the ropes as "distributed masses" and the respectively loaded or empty tubs as concentrated masses.

On the other hand, some mechanical properties of the assembly e.g. the rigidity of particular elements are differ considerably. It could be then accepted that rotating masses and tubs are ideal rigid bodies whilst supporting and balance ropes are flexible parts of the assembly.

Considering the case shown in Fig. 1, which is the most interesting for practical purposes in operational situations of skip tubs, i.e. when one tub is near the shaft top and the other is approaching the shaft's bottom (braking being applied as the filled tub approaches the shaft top) the hoist could be substituted by the model presented in Fig. 2 (Wolny, 2000 a, Wolny 2000 b).

In this model we have:

$$M_0 = \frac{G_0}{g}, \qquad M_i = \frac{1}{g}(G_1 + q_1 \cdot l_i) \qquad (i = 1, 2),$$

where: G_1, G_2, G_0 — the weights of tubs and the reduced weigh of rotating elements of the hoist including the guide wheels. Masses of short parts of ropes l_1 (between the upper tub and the drive wheel) and l_2(below the bottom tub near the reverse in the sump) are, for purposes of calculation, included in the masses of the tubs.

The following simplifications have been made to the model presented in Fig. 2 (Knop, 1975), (Wolny, 1987):

— the drive wheel, rope wheels and armatures of electric motors are considered as a single rigid mass of the $M.I.I_0 = I_L + I_N + I_s$ due to the high torsional rigidity of the short drive shaft and the considerations give in (Knop, 1975),

— both tubs are considered as rigid bodies,

— structural damping in ropes is negleced due to the short time of the operational braking process,

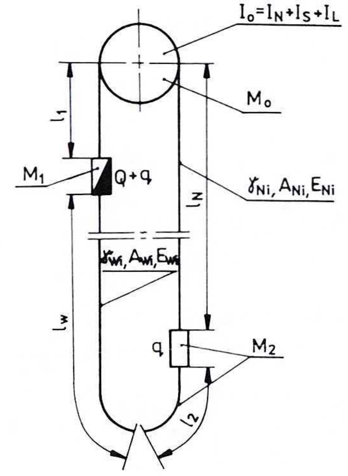

Fig. 2. The model of the hoist facility

— vibrations from one side are no transferred across the balance rope loop onto the other side; thus a closed assembly of model masses (Fig. 2) could be isolated under this circumstance.

The assembly from Fig. 2 could be described, after rationalisation (Fig. 3) as a one — dimensional, inertial system of a finite number of concentrated rigid masses located along a straight line and the elastic masses distributed in a continuous mode.

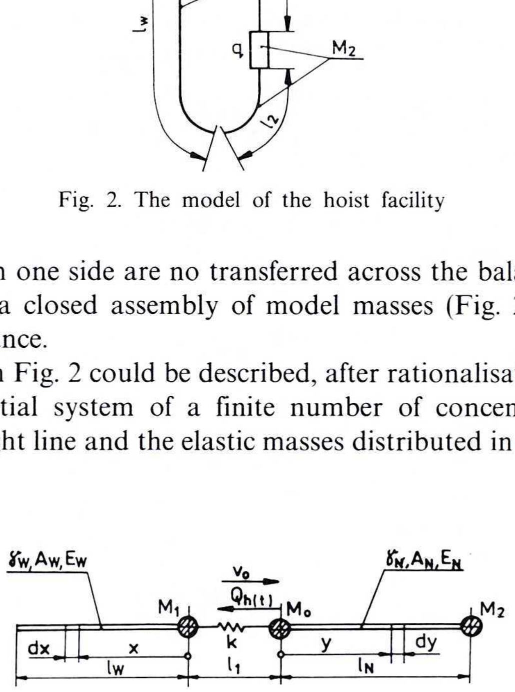

Fig. 3. The model of hoist facility the case of operational braking condition after straghtening: $Q_{h(t)}$ — braking force in the drive sheel, M_1 — mass of the tub with the output, M_0 — reduced masses rotating in the tower, M_2 — reduced masses of the hoist in the sump, l_1 — length of supporting ropes between the upper tub and the drive wheel, l_w — length of balance ropes, l_N — length of supporting ropes, $A_W E_W$, $A_N E_N$ — tension rigidity of balance ropes and supporting ropes, γ_W, γ_N — linear density of balance ropes and supporting ropes

In this model — where the reaction of the short element of the balance rope l_2 from the reverse to the bottom tub is negligibly small — the mass of this part has been included into the mass of the tub.

$$M_2 = q + \gamma_w \cdot l_2. \tag{1}$$

The model, strucured in this pattern has been verified so long as the total axial force in any cross-section of the rope exceeds zero.

Masses M_0 and M_1 relate to the weightless spring of the elasticity coefficient:

$$k = \frac{A_N E_N}{l_1} \tag{2}$$

which is equal to the elasticity on the section of the supporting ropes between from the upper tub and the drive wheel.

2. Operational braking of the mining hoist

The operational braking effect of the mining hoist is the result of the action of the force exerted by the exerted braking applied to the drive wheel (in Fig. 3 the force $Q_{h(t)}$ is applied to the mass M_0).

Dispalcements and strains of cross-sections of supporting and balance ropes after the initiation of the operational braking process could be determined after solution of the following equations:

$$\begin{gathered}\frac{\partial^2 u(x,t)}{\partial t^2} - a_w^2 \frac{\partial^2 u(x,t)}{\partial x^2} = 0, \\ \\ \frac{\partial^2 v(y,t)}{\partial t^2} - a_N^2 \frac{\partial^2 v(y,t)}{\partial y^2} = 0,\end{gathered} \tag{3}$$

within the boundary conditions:

$$x = 0, \quad M_1 \frac{\partial^2 u}{\partial t^2} = A_w E_w \frac{\partial u}{\partial x} - k\left[u(x=0,t) + v(y=0,t)\right], \tag{4a}$$

$$x = l_w, \quad \frac{\partial u}{\partial x} = 0, \tag{4b}$$

$$y = 0, \quad M_0 \frac{\partial^2 v}{\partial t^2} = A_N E_N \frac{\partial v}{\partial y} - k\left[u(x=0,t) + v(y=0,t)\right] - Q_h(t), \tag{4c}$$

$$y = l_N, \quad M_2 \frac{\partial^2 v}{\partial t^2} = -A_N E_N \frac{\partial v}{\partial y} \tag{4d}$$

and assuming zero initial conditons.

In the above relations we have: $u(x,t)$, $v(y,t)$ — displacements of any cross-section of ropes within a distance (for $t = 0$) x, y from the origins of movable co-ordinate systems connected with the masses M_1 or M_0; displacements are calculated for systems whose origins at the moment $t = 0$ were identical with masses M_1 and M_0 and they move with the velocity $v_0 = \text{const}$, which is assumed to be the same as the velocity of all elements of the hoist at the initial moment, $Q_{h(t)}$ — i.e. when the braking force is applied to the assembly.

The step mode of application of the force $Q_h = \text{const}$ to the assembly that has been analysed in published literature (Knop, 1975), (Wolny, 2000 a), (Wolny, 2000 b) is somewhat of theoretical significance. The calculations of loads in tub suspensions and balance ropes made due to such a method of application of braking force gave immoderately high results, which have not been confirmed in practice. A number of

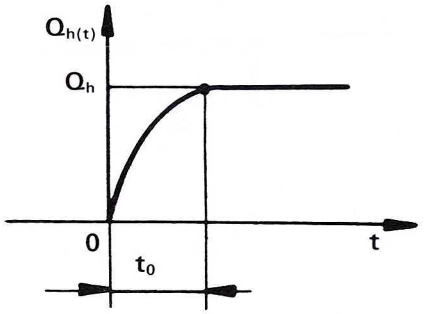

Fig. 4. Function of exciting fores

measurements performed in the field — (Knop, 1975), as well as measurements of the pressure fluctuation in the cylinder of the operational brake (Śmieja, 2000) gave the good reason to approximate the curve from Fig. 4 by an equation of the type:

$$Q_{h(t)} = 2Q_h(1 - e^{-a_0 f}) \quad \text{for} \quad t \in (0, t_0), \tag{5a}$$

and

$$Q_{h(t)} = Q_h \quad \text{for} \quad t \in (t_0, \infty), \tag{5b}$$

where: a_0 — index exponent.

The solution of equations (3) is expected to have the form (Wolny, 1999), (Wolny, 2000 b):

$$u(x, t) = \varphi\left(t - \frac{x}{a_N}\right) + \psi\left(t + \frac{x}{a_w}\right), \tag{6a}$$

$$v(y, t) = f\left(t - \frac{y}{a_N}\right) + \vartheta\left(t + \frac{y}{a_w}\right), \tag{6b}$$

With regarding to (6a) and (6b) in equations (3) and in the boundary conditions (4) the forms of functions φ, ψ, f, and ϑ have been determined for different intervals of variables y, t and x, t. It enabled the formulation of general analytical formulae determining displacements and stresses in the supporting and balance ropes (Wolny, 2000).

Displacements are described by the formulae:

— for the balance rope

$$u(x,t) = \frac{2Q_h A_N E_N}{M_0 \cdot M_1 l_1}\left[q_{01}\left(t - \frac{x}{a_W}\right) + q_{02} + \sum_{i=0}^{3} q_i e^{a_i\left(t - \frac{x}{a_W}\right)}\right], \tag{7a}$$

— for the supporting rope

$$v(y,t) = \frac{2Q_h}{M_0 \cdot M_1}\left[W_{01}\left(t - \frac{y}{a_N}\right) + W_{02} + \sum_{i=0}^{3} W_i e^{a_i\left(t - \frac{y}{a_N}\right)}\right], \tag{7b}$$

where:

$$q_{01} = \frac{M_0 M_1 l_1}{A_N E_N\left(\frac{A_N E_N}{a_N} + \frac{A_W E_W}{a_W}\right)}, \tag{8a}$$

$$q_{02} = \frac{-M_0 l_1}{A_N E_N\left(\frac{A_N E_N}{a_N} + \frac{A_W E_W}{a_N}\right)}\left[\frac{1}{a_0} + \frac{M_0 + M_1 + \frac{A_W E_W}{a_N a_W} l_1}{\frac{A_N E_N}{a_N} + \frac{A_W E_W}{a_W}}\right], \tag{8b}$$

$$q_0 = \frac{-1}{a_0(a_0^3 - A_0^2 + B a_0 - C)}, \tag{8c}$$

$$q_1 = \frac{a_0(a_i - a_i)}{a_i^2(a_i + a_0)(a_i - a_1)(a_i - a_2)(a_i - a_3)} \quad (i = 1, 2, 3), \tag{8d}$$

$a_i(1,2,3)$ — are the roots of the equation

$$a^3 + Aa^2 + Ba + C = 0, \tag{9}$$

$$A = \frac{A_N E_N}{M_0 a_N} + \frac{A_W E_W}{M_1 a_W}, \qquad B = \frac{A_N E_N}{M_0 a_N}\frac{A_W E_W}{M_1 a_W} + \frac{A_N E_N}{M_0 M_1 l_1}(M_0 + M_1),$$

$$C = \frac{A_N E_N}{M_0 M_1 l_1}\left(\frac{A_N E_N}{a_N} + \frac{A_W E_W}{a_W}\right)$$

and

$$W_{01} = \frac{-M_0 M_1}{\frac{A_N E_N}{a_N} + \frac{A_W E_W}{a_N}}, \tag{10a}$$

$$W_{02} = \frac{M_0 M_1 l_1}{\left(\frac{A_N E_N}{a_N} + \frac{A_W E_W}{a_W}\right)}\left[\frac{\frac{M_0 M_1}{l_1} + \frac{A_W E_W}{a_N a_W}}{\frac{A_N E_N}{a_N} + \frac{A_W E_W}{a_W}} + \frac{1}{a_0 l_1} - \frac{1}{a_W}\frac{A_W E_W}{A_N E_N}\right], \tag{10b}$$

$$W_0 = \frac{M_1 a_0^2 - \frac{A_W E_W}{a_W} a_0 + \frac{A_N E_N}{l_1}}{a_0(a_0^3 - A_0^2 + Ba_0 - C)}, \tag{10c}$$

$$W_i = \frac{-a_0\left(M_1 a_i^2 + \frac{A_W E}{a_W} a_i + \frac{A_N E_N}{l_1}\right)(a_i - a_i)}{a_i^2(a_i + a_0)(a_i - a_1)(a_i - a_2)(a_i - a_3)} \quad (i = 1, 2, 3). \tag{10d}$$

Analytical formulae (7a) and (7b) determining displacements in any cross-section of supporting ropes and balance ropes made it possible to formulate relations that lead to the determination of the load of any cross-section of ropes including loads of tubs suspension and balance ropes:

a) suspension of the upper tub

$$S_{l_N} = k\left[u(x=0,t) + v(y=0,\mathrm{t})\right] = \frac{A_N E_N}{l_1}\left\{\frac{2Q_h A_N E_N}{M_0 M_1 l_1}\left[q_{01}t + q_{02} + \sum_{i=0}^{3} q_i e^{a_i t}\right] + \right.$$
$$\left. + \frac{2Q_h}{M_0 M_1}\left[W_{01}t + W_{02} + \sum_{i=0}^{3} W_i e^{a_i t}\right]\right\}, \tag{11}$$

b) suspension of the balance rope

$$S_{l_W} = A_W E_W \frac{\partial u(x=0,t)}{\partial x} = -\frac{2Q_h}{M_0 M_1}\frac{A_N E_N}{l_1}\frac{A_W E_W}{a_W}\left[q_{01} + \sum_{i=1}^{3} a_i q_i e^{a_i t}\right], \tag{12}$$

c) suspension of the bottom tub

$$S_{l_{ND}} = A_N E_N \frac{\partial v(y=l_N,t)}{\partial y} = -\frac{2Q_h}{M_0 M_1}\frac{A_N E_N}{a_N}\left[W_{01} + \sum_{i=0}^{3} a_i W_i e^{a_i\left(t - \frac{l_N}{a_N}\right)}\right]. \tag{13}$$

Fig. 5 shows an exemplary diagram illustrating the change of load of the upper tub (filled and approaching the upper loading level) at the stage of operational braking (relation 11). The experiment was made with a winding facility of the following parameters:

— reduced masses rotating in the tower; $M_0 = 40000$ [kg],
— tension rigidity of supporting ropes; $A_N E_N = 308$ [MN],
— distance between the upper tub and the drive wheel; $l_1 = 100$ [m].

The drive wheel was arrested by the a facility of the following parameters (relation (5) and Fig. 4): $Q_h = 248$ [kN], $t_0 = 0.9$ [s], $a_0 = 2.11$ [1/s] and with variable masses of the tub: $M_1 = 30000$ [kg], 35000 [kg], 40000 [kg], 45000 [kg], and 50000 [kg].

The curves illustrate the change of load in the suspended tub for subsequent values of the ratio $C = M_0/M_1$: namely: 1.33, 1.14, 1.00, 0.89, and 0.80.

The below simplification have been assumed (for the "tower" hoist):

$$\frac{A_W E_W}{a_W} = \frac{A_N E_N}{a_N} = \frac{AE}{a}, \quad \text{and} \quad M_0 \cong M_1 = M \tag{14}$$

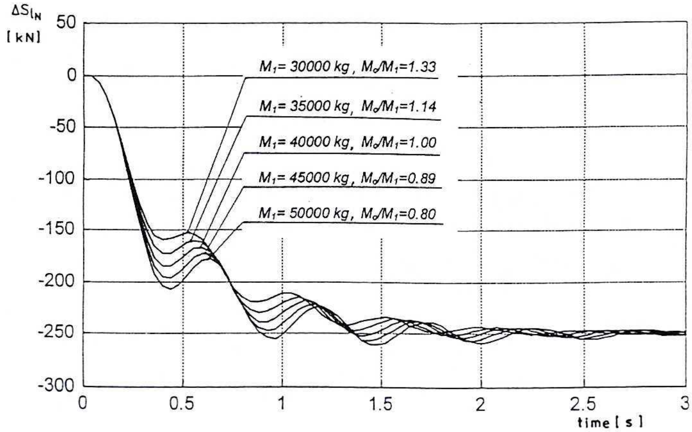

Fig. 5. Changes of load of the upper tub suspension (filled) reaching the upper unloading level at the time of operational braking and the steady braking force ($Q_h = 248$ [kN], $t_0 = 0{,}9$ [s], $a_0 = 2.11$ [1/s])

and the following solutions were obtained:

a) displacement of cross-sections of balance ropes

$$u^*(x,t) = \frac{2Q_h}{M^2}\frac{AE}{l_1}\left\{\frac{M^2 l_1 a}{2(AE)^2}\left(t-\frac{x}{a_W}\right) - \frac{M^2 l_1}{2(AE)^2}\left[\frac{a}{a_0}+\frac{l_1}{2}+\frac{a^2 M}{AE}\right]+\right.$$

$$+\frac{e^{-a_0\left(t-\frac{x}{a_W}\right)}}{a_0\left\{a_0^3-2\frac{AE}{Ma}a_0^2+\left[\left(\frac{AE}{Ma}\right)^2+\frac{2AE}{Ml_1}\right]a_0-2\frac{(AE)^2}{M^2 l_1 a}\right\}}-\frac{a_0 e^{-\frac{AE}{Ma}\left(t-\frac{x}{a_W}\right)}}{2\left(\frac{AE}{Ma}\right)^2\left(\frac{AE}{Ma}-a_0\right)\frac{AE}{Ml_1}}+$$

$$+\frac{a_0\sqrt{2\frac{AE}{Ml_1}}e^{-\frac{AE}{2Ma}\left(t-\frac{x}{a_W}\right)}}{4\left(\frac{AE}{Ml_1}\right)^2\sqrt{2\frac{AE}{Ml_1}+a_0\left(a_0+\frac{AE}{Ma}\right)}\sqrt{2\frac{AE}{Ml_1}-\left(\frac{AE}{2Ma}\right)^2}}\times$$

$$\left.\times\sin\left[\sqrt{2\frac{AE}{Ml_1}-\left(\frac{AE}{2Ma}\right)^2}\left(t-\frac{x}{a_W}\right)+\Phi\right]\right\}, \tag{15}$$

$$\Phi = \frac{\pi}{2} - \operatorname{arctg}\left\{ \frac{\frac{AE}{2Ma}\left(a_0 + \frac{AE}{Ma}\right) - 2\frac{AE}{Ml_1}}{\left(a_0 + \frac{AE}{Ma}\right)\sqrt{2\frac{AE}{Ml_1} - \left(\frac{AE}{2Ma}\right)^2}} \right\}.$$

b) displacement of cross-sections of supporting ropes

$$v^*(y,t) = \frac{2Q_h}{M^2}\left\{ -\frac{M^2 a}{2AE}\left(t - \frac{y}{a_N}\right) + \frac{M^2 l_1 a}{2AE}\left(\frac{Ma}{l_1 AE} - \frac{1}{2a} + \frac{1}{a_0 l_1}\right) + \right.$$

$$+ \frac{Ma_0^2 + AE\left(\frac{a_0}{a} + \frac{1}{l_1}\right)}{a_0\left[a_0^3 - 2\frac{AE}{Ma}a_0^2\left[\left(\frac{AE}{Ma}\right)^2 + 2\frac{AE}{Ml_1}\right]a_0 + 2\left(\frac{AE}{Ma}\right)^2\frac{a}{l_1}\right]} e^{-a_0\left(t - \frac{y}{a_N}\right)} -$$

$$- \frac{Ma_0}{2\left(\frac{AE}{Ma}\right)^2\left(\frac{AE}{Ma} + a_0\right)} e^{-\frac{AE}{Ma}\left(t - \frac{y}{a_N}\right)} + \frac{Ma\sqrt{2\frac{AE}{Ml_1}\cdot e^{-\frac{AE}{2Ma}\left(t - \frac{y}{a_N}\right)}}}{4\frac{AE}{Ml_1}\sqrt{2\frac{AE}{Ml_1} + a_0\left(a_0 + \frac{AE}{Ma}\right)}\sqrt{2\frac{AE}{Ml_1} - \left(\frac{AE}{2Ma}\right)^2}}\cdot$$

$$\left.\cdot \sin\left[\sqrt{\frac{AE}{Ml_1} - \left(\frac{AE}{2Ma}\right)^2}\left(t - \frac{y}{a_N}\right) + \Phi\right]\right\}. \qquad (16)$$

— Moreover, the stress in any cross-section of ropes could be determined from the following relationships:

a) for the balance rope

$$\sigma^*(x,t) = \frac{-2EQ_h}{a_W M^2}\left\{ \frac{M^2 a}{2AE} - \frac{\frac{AE}{l_1} e^{-a_0\left(t - \frac{x}{a_W}\right)}}{\left[a_0^3 + 2\frac{AE}{Ma}a_0^2 + \left[\left(\frac{AE}{Ma}\right)^2 + \frac{2AE}{Ml_1}\right]a_0 + 2\frac{(AE)^2}{M^2 l_1 a}\right]} + \right.$$

$$- \frac{\mathrm{M}\cdot \mathrm{a}_0 \mathrm{e}^{-\frac{AE}{2Ma}\left(t - \frac{x}{a_W}\right)}}{2\frac{AE}{Ma}\left(\frac{AE}{Ma} + a_0\right)} - \frac{M\cdot a_0 e^{-\frac{AE}{2Ma}\left(t - \frac{x}{a_W}\right)}}{2\sqrt{2\frac{AE}{Ml_1} + a_0\left(a_0 + \frac{AE}{Ma}\right)}\sqrt{2\frac{AE}{Ml_1} - \left(\frac{AE}{2Ma}\right)^2}}\cdot$$

$$\left.\cdot \sin\left[\sqrt{2\frac{AE}{Ml_1}-\left(\frac{AE}{2Ma}\right)^2}\left(t-\frac{x}{a_W}\right)+\Phi_1^*\right]\right\}, \quad (17)$$

where:

$$\Phi_1=\frac{\pi}{2}-\operatorname{arctg}\left\{\frac{a_0+\frac{AE}{2Ma}}{\sqrt{2\frac{AE}{ML_1}-\left(\frac{AE}{2Ma}\right)^2}}\right\}$$

b) for the supporting rope

$$\sigma^*(y,t)=\frac{-2EQ_h}{M^2a_N}\left\{\frac{M^2a}{2AE}-\frac{\left[Ma_0^2+AE\left(\frac{a_0}{a}+\frac{1}{l_1}\right)\right]e^{a_0\left(t-\frac{y}{a_N}\right)}}{\left[a_0^3+2\frac{AE}{Ma}a_0^2+\left[\left(\frac{AE}{Ma}\right)^2+\frac{AE}{Ml_1}\right]a_0+2\left(\frac{AE}{Ma}\right)^2\frac{a}{l_1}\right]}-\right.$$

$$-\frac{Ma_0}{2\left(\frac{AE}{Ma}\right)\left(a_0+\frac{AE}{Ma}\right)}e^{-\frac{AE}{Ma}\left(t-\frac{y}{a_N}\right)}+$$

$$+\frac{M\cdot a_0e^{-\frac{AE}{2Ma}\left(t-\frac{y}{a_N}\right)}}{2\sqrt{2\frac{AE}{Ml_1}+a_0\left(a_0+\frac{AE}{Ma}\right)}\sqrt{2\frac{AE}{Ml_1}-\left(\frac{AE}{2Ma}\right)^2}}-$$

$$-\frac{Ma_0}{2\left(\frac{AE}{Ma}\right)\left(a_0+\frac{AE}{Ma}\right)}e^{-\frac{AE}{Ma}\left(t-\frac{y}{a_N}\right)}+$$

$$+\frac{Ma_0e^{-\frac{AE}{2Ma}\left(t-\frac{y}{a_N}\right)}}{2\sqrt{2\frac{AE}{Ml_1}+a_0\left(a_0+\frac{AE}{Ma}\right)}\sqrt{2\frac{AE}{Ml_1}-\left(\frac{AE}{2Ma}\right)^2}}\times$$

$$\left.\times\sin\left[\sqrt{2\frac{AE}{Ml_1}-\left(\frac{AE}{2Ma}\right)^2}\left(t-\frac{y}{a_N}\right)+\Phi_1\right]\right\} \quad (18)$$

The load of the upper tub suspension loaded may be determined from the relationship:

$$S^*_{L_N} = k\left[u^*(x=0,t)+v^*(y=0,t)\right] =$$

$$= \left\{ \frac{-\sqrt{2\frac{AE}{Ml_1}}a_0 e^{-\frac{AE}{2Ma}t}}{\sqrt{2\frac{AE}{Ml_1}+a_0\left(a_0+\frac{AE}{Ma}\right)}\sqrt{2\frac{AE}{Ml_1}-\left(\frac{AE}{2Ma}\right)^2}} \sin\left(\sqrt{2\frac{AE}{Ml_1}-\left(\frac{AE}{Ml_1}\right)^2}t+\Phi\right)+ \right.$$

$$\left. + \frac{2\frac{AE}{ML_1}e^{a_0 t}}{\left[a_0^2+\frac{AE}{Ma}a_0+2\frac{AE}{Ml_1}\right]} - 1 \right\}. \quad (19)$$

Moreover, the force in the supporting rope at the point of disengagement with the drive wheel ($y=0$) is:

$$S^*_{L_{N(y=0)}} = AE\frac{\partial v(y=0,t)}{\partial y} = \frac{2AEQ_h}{M^2 \cdot a_N}\left\{ \frac{M^2 a}{2AE} - \frac{\left[Ma^2+AE\left(\frac{a_0}{a}+\frac{1}{l_1}\right)\right]e^{a_0 t}}{\left(a_0+\frac{AE}{Ma}\right)\left[a_0\left(a_0+\frac{AE}{Ma}\right)+2\frac{AE}{Ml_1}\right]} - \right.$$

$$-\frac{Ma_0 e^{-\frac{AE}{Ma}t}}{2\left(\frac{AE}{Ma}\right)+\left(a_0+\frac{AE}{Ma}\right)}+$$

$$+\frac{M\cdot a_0 e^{-\frac{AE}{2Ma}t}}{2\sqrt{2\frac{AE}{2l_1}+a_0\left(a_0+\frac{AE}{Ma}\right)}\sqrt{2\frac{AE}{2Ml_1}-\left(\frac{AE}{2Ma}\right)^2}}\cdot$$

$$\left. \cdot\sin\left(\sqrt{2\frac{AE}{Ml_1}-\left(\frac{AE}{2Ma}\right)^2}t+\Phi_1\right]\right\}. \quad (20)$$

The force in the bottom tub suspension ($y = l_N$) is:

$$S^*_{l_N(y=l_N)} = AE\frac{\partial v(y = l_N, t)}{\partial y} = \frac{2AE \cdot Q_h}{M^2 a_N}\left\{\frac{M^2 a}{2AE} - \frac{\left[Ma^2 + AE\left(\frac{a_0}{a} + \frac{1}{l_1}\right)\right] e^{a_0\left(t - \frac{l_N}{a_N}\right)}}{\left(a_0 + \frac{AE}{Ma}\right)\left[a_0\left(a_0 + \frac{AE}{Ma}\right) + 2\frac{AE}{Ml_1}\right]} - \right.$$

$$- \frac{M \cdot a_0 e^{-\frac{AE}{Ma}\left(t - \frac{l_N}{a_N}\right)}}{2\left(\frac{AE}{Ma}\right) + \left(a_0 + \frac{AE}{Ma}\right)} + \frac{Ma_0 e^{-\frac{AE}{2Ma}}}{2\sqrt{2\frac{AE}{Ml_1} + a_0\left(a_0 + \frac{AE}{Ma}\right)}\sqrt{2\frac{AE}{Ml_1} - \left(\frac{AE}{2Ma}\right)^2}} \times$$

$$\left. \times \sin\left(\sqrt{2\frac{AE}{Ml_1} - \left(\frac{AE}{2Ma}\right)^2}\left(t - \frac{l_N}{a_N}\right) + \Phi\right]\right\} \quad (21)$$

The load of the upper tub suspension — according to formulae (11) and (19) — has been reduced by the braking operation (it is unloaded). It should be noted that the change of the load does not depend solely on the structure of the assembly in use, but is also dependent on the parameters of the braking force.

Generally, the operational braking process, according to a fatigue-strength calculation could be analysed by introducing into the load cycle of the tub suspension an additional single load of values within its working minimum and maximum (Wolny & Dzik, 1998).

Results obtained in theoretical considerations, which describe the process of operational braking, have been verified by mesurements of selected data in the real object practice. Owing to some technological difficulties the experiment was limited to the measurement of forces in the suspension of a filled tub approaching the upper loading level and slowed by the operational brake (Śmieja, 2000).

3. Measurements of forces in the tub suspension made in practice during operational braking of the real object

3.1. General technological data of the hoist where the experiment was performed

General technological data of the hoist installation:

Type of machine	4L-4000/2900
Drive	D/C motor; 2900 kW
Rated revolutions	77 rpm
Maximum rate of ascent	$v = 16$ [m/s]
Mass of the assembled empty tub including its suspension	$m_{ku} = 16500$ [kg]

Effective mass	$m_{ku} = 1700$ [kg]
Depth of winding	$H = 1040$ [m]
Moments of inertia of rotating elements (GD^2)	
a) flywheel effect of the drum	$GD_s^2 = 1868.8$ [kNm^2]
b) flywheel effect of the motor rotor	$GD_s^2 = 1275.3$ [kNm^2]
c) flywheel effect of the guide wheels	$GD_s^2 = 427$ [kNm^2]

3.2. The measuring apparatus for recording forces in the tub suspension ropes

The scheme of the measuring apparatus for recording forces in the suspensions of tubs is shown in Fig. 6. To obtain measurements strain gauge sensors "WSP" of the following technical data were employed (Śmieja, 2000):

Measurement range -100 kN

Output voltage -5 v

Quality rating $\pm 0.6\%$

Bridge voltage -5 V

Signals were recorded using a ZPR-1 set with a HP battery power source (2.6—12v). Measurement signals were gathrered from eight sensors (two to each rope), and were sampled at a frequency of 40 kHz. The signals recorded from each channel were converted to text files then summed-up and finally processed using the computer programme *Matlab5.2*. Peripheral velocities of the drive wheel were recorded in all measurements.

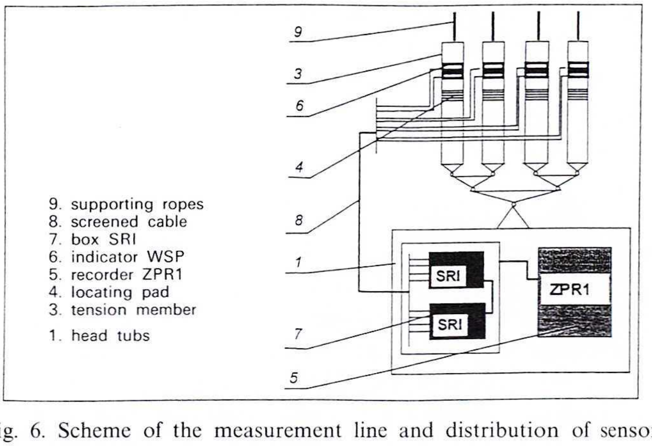

Fig. 6. Scheme of the measurement line and distribution of sensors

3.3. Results of measurements of forces in tub suspensions in the operational braking state

In this part of the paper the results of measurements of forces in the suspension of the tub approaching the shaft top in the condition of operational braking of the hoist facility of above described technological parameters are presented. Dotted line in

Fig. 7 represents the real load of the tub suspension approaching the shaft top ($l_1 = 100$ m) in the time of operational braking.

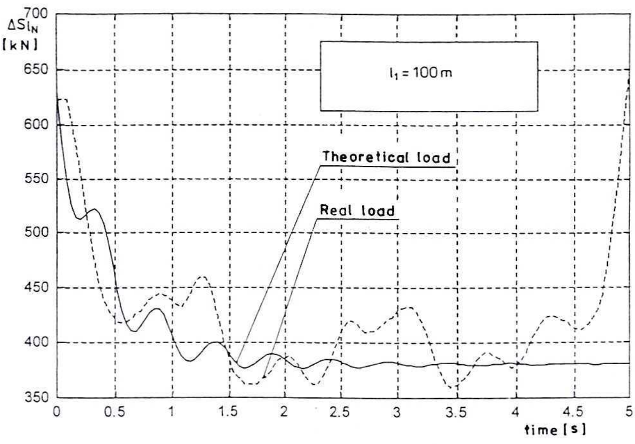

Fig. 7. Diagram of change of the tub load in the condition of operational braking for the distance between the tub and the drive wheel $l_1 = 100$ [m]
— load obtained in theoretical consideration (continuous line)
— real load of the tub obtained in measurement (dotted line)

The braking assembly of the characteristics presented in Fig. 4 and described by the relation (5) braked the hoist facility. Parameters of the braking assembly have been determined on the base of the technological documentation of the facility (Śmieja, 2000), and results of pressure measurements in the braking assembly cylinder. Its characteristic data obtained in calculations are:

— braking force $Q_h = 248$ [kN]
— $a_0 = 2.11$ [1/s]
— $t_0 = 0.90$ [s].

The continuous line shows the change of load of the tub suspension obtained from, theoretical analysis (relation (11)).

Similarly in Fig. 8 is presented the change of load of the tub suspension obtained from measurements (dotted line) in the condition of operational braking for the length of supporting rope between the filled tub and the drive wheel $l_1 = 820$ [m] realised by the braking assembly as in the previous case. The change of load of the tub suspension obtained in theoretical consideration is presented by continuous line (as in previous case).

Measurements made in the final stage of the operational braking show the significant increase of the tub suspension load that could be seen in the present diagrams (Fig. 7 and Fig. 8). As a matter of fact it is the result of the additional loading of the tub suspension owing to elastic deformation of ropes after the drive wheel stoppage.

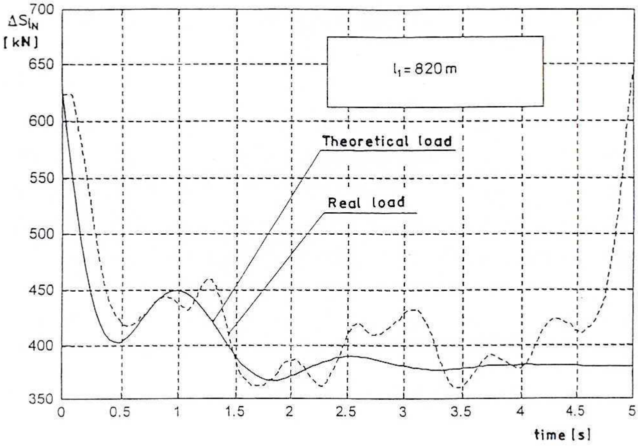

Fig. 8. Diagram of change of the tub load in the condition of operational braking for the distance between the tub and the drive wheel $l_1 = 820$ [m]
— load obtained in theoretical consideration (continuous line)
— real load of the tu obtained in measurement (dotted line)

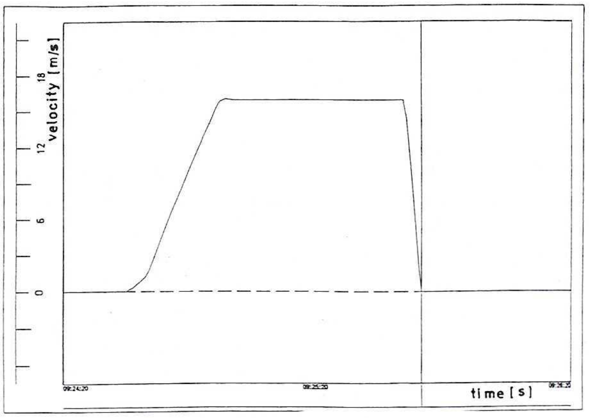

Fig. 9. Run diagram made at the time of testing the suspension load in condition of operational braking

Moreover in Fig. 9 is presented the diagram of the tub travel made at the time of testing the load in the tub suspension in operational braking condition at the stabilised running velocity of the tub $v = 16$ [m/s].

4. Conclusions

The results of measurements (in this paper limited to the measurement of forces in the tub suspension) correspond to the predicted theoretical values based on the dynamic analysis presented in this paper. Differences in typical values for the process of operational braking may be seen in the time function diagrams of the measured and theoretically determined forces in suspensions of tubs do not exceed, even in extreme cases, a few percent (see diagrams Fig. 7, Fig. 8).

The results obtained form a starting point for a fundamental description of the function, showing the changing loadings of parts of the tub-hauling assembly during the braking process. These are dependant on the design parameters of the pit-head assembly as well as the braking mechanism itself. Such relationships are necessary in the general design process and specifically in the design of the frictional coupling between the rope and the drive wheel. Moreover they are one of the fundamental factors for the evolution of criteria governing the design of mining tubs with a view to ensuring optimal safety and operational reliability. (obligatory regulations, see: Enclosure)

REFERENCES

Gerlich A, Horstmann E.; 1993. Seilrutschverhalten von Treibscheibenanlagen unter Berücksichtigung dynamischer Vorgänge. Glückauf — Forschunashefte 54, nr 5. ss. 213÷218.

Knop H.; 1975. Wybrane zagadnienia z dynamiki urządzeń wyciągowych. ZN AGH. Elektryfikacja i Mechanizacja Górnictwa i Hutnictwa. Z. 67. Kraków ss. 1÷103.

Śmieja M.; 2000. Analityczna i eksperymentalna ocena współczynników bezpieczeństwa wybranych elementów kopalnianego urządzenia wyciągowego. Praca doktorska. AGH. nie publikowana. Kraków. ss. 1÷88.

Wolny S.; 1987. Teoretyczne rozważania nad procesem hamowania krańcowego naczyń wydobywczych wyciągów kopalnianych. ZN. AGH. Mechanika. Z. 11. Kraków. ss. 1÷109.

Wolny S., Dzik S.; 1998. Badanie stanu naprężenia w elementach zawieszeń górniczych urządzeń wyciągowych. XIII Sympozjum Mechaniki Eksperymentalnej Ciała Stałego. Jachranka. ss. 455÷460.

Wolny S.; 1999. Analiza dynamiczna i wytrzymałościowa pracy zawieszeń naczyń oraz lin wyrównawczych w aspekcie opracowania kryteriów ich projektowania i eksploatacji. Projekt badawczy KBN (Umowa Nr 371/T12/97/13). nie publikowana. Kraków. ss. 1÷123.

Wolny S.; 2000 a. Obciążenia dynamiczne w zawieszeniach naczyń wydobywczych i lin wyrównawczych w warunkach hamowania bezpieczeństwa górniczego urządzenia wyciągowego. ZN AGH. Kwartalnik Mechanika. T. 19. Z. 1. Kraków. ss. 121÷130.

Wolny S., 2000 b. Wybrane problemy dynamiczne i wytrzymałościowe w eksploatacji górniczych urządzeń wyciągowych. Monografie „Problemy Inżynierii Mechanicznej i Robotyki" Nr 1. Wyd. Wydział Inżynierii Mechanicznej i Robotyki. AGH. Kraków. ss. 1÷123.

Załącznik nr 17 do rozporządzenia Ministra Przemysłu i Handlu z dnia 14.04.1995. „Wymagania w zakresie budowy i obsługi górniczych wyciągów szybowych".

REVIEW BY: PROF. DR HAB. INŻ. TADEUSZ BANASZEWSKI, KRAKÓW

Received: 07 August 2000.